

The role of Coulomb correlation in charge density wave of CuTe

Sooran Kim¹, Bongjae Kim^{2,3}, and Kyoo Kim^{3*}

¹*Department of Physics Education,
Kyungpook National University, Daegu 41566, Korea*

²*Department of Physics,
Kunsan National University, Gunsan 54150, Korea*

³*Max Planck POSTECH/Hsinchu Center for Complex Phase Materials,
Pohang University of Science and Technology,
Pohang 37673, Korea*

(Dated: March 10, 2022)

A quasi one-dimensional layered material, CuTe undergoes a charge density wave (CDW) transition in Te chains with a modulation vector of $q_{CDW} = (0.4, 0.0, 0.5)$. Despite the clear experimental evidence for the CDW, the theoretical understanding especially the role of the electron-electron correlation in the CDW has not been fully explored. Here, using first principles calculations, we demonstrate the correlation effect of Cu is critical to stabilize the $5 \times 1 \times 2$ modulation of Te chains. We find that the phonon calculation with the strong Coulomb correlation exhibits the imaginary phonon frequency so-called phonon soft mode at $q_{ph0} = (0.4, 0.0, 0.5)$ indicating the structural instability. The corresponding lattice distortion of the soft mode agrees well with the experimental modulation. These results demonstrate that the CDW transition in CuTe originates from the interplay of the Coulomb correlation and electron-phonon interaction.

I. INTRODUCTION

The novel electronic and magnetic properties of low dimensional materials have drawn interest because of their fundamental physics and possible applications^{1–6}. The intrinsic instabilities in low dimensional systems often trigger charge density wave (CDW), Peierls transitions, spin density wave, or even unconventional superconductivity^{7–11}. Peierls-type transitions are experimentally observed in quasi one-dimensional (1D) materials such as TTF-TCNQ molecular solid *trans*-polyacetylene polymers, MQ_3 ($M=\text{Ta, Nb}$ and $Q=\text{S, Se}$), $\text{K}_{0.3}\text{MoO}_3$ ^{12–20} (see Table I within Ref. 15).

Electronic instability, however, widely understood as the origin of a Peierls transition, has been challenged^{10,11,23,24}. As the dimension of interatomic connection increases, the susceptibility peak feature becomes weaken, and other mechanisms such as electron-phonon interaction become important in the realization of a Peierls-type structural, or CDW transition. Sometimes, the role of the underlying 1D interatomic network can be pronounced due to the directional bonding, for instance, of p orbitals in elements such as Se, Te, and I, resulting in strong 1D Peierls-type structural transitions in higher dimensions^{21,22}. Furthermore, even though the Peierls transition does not require the strong electron-electron correlation as in the Mott transition, there have been reports on the role of strong Coulomb correlation in the Peierls transition, dubbed as a Mott-Peierls transition, especially, in VO_2 ^{25–30}. Therefore elucidating the mechanism of CDW transitions, which can be originated from the Fermi surface nesting, electron-phonon interaction, electron-electron correlation, or even the interplay of them would be interesting and important for fundamental physics in low dimensional systems.

The crystal CuTe, called vulcanite, is one of the prototypical quasi 1D systems, which undergoes a CDW transition at $T_{CDW} = 335$ K. The early X-ray diffraction study reported that CuTe is crystallized in the strained FeTe-like orthorhombic unit cell with the space group $Pmmn$ (No. 59) which consists of one formula unit of CuTe³¹. As shown in Fig. 1(a) and (b), Te atoms form

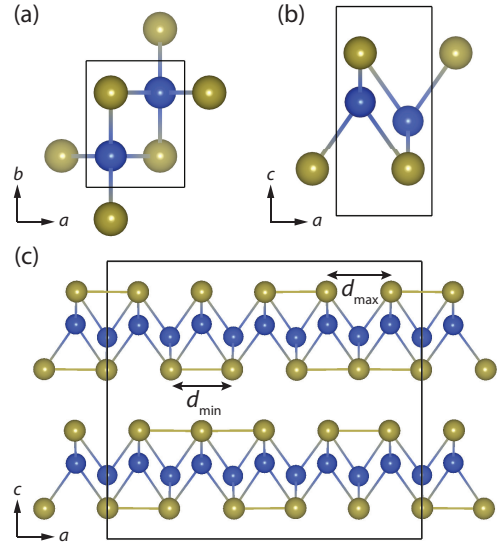


FIG. 1: Crystal structures of CuTe. Blue and yellow balls represent Cu and Te, respectively. (a) high symmetric structure in the non-CDW phase at a high temperature. (b) $5 \times 1 \times 2$ modulated structure in the CDW phase. The bond between Te atoms illustrates the Te modulation along the a direction reported in REF. 33,34. d_{min} and d_{max} indicate the shortest and longest distances among Te-Te bondings, respectively.

a distorted square planar net resulting in the quasi 1D chain structure, and Cu atoms have a planar square network with buckling in the non-CDW phase of CuTe.

According to the tight binding calculation of Seong *et al.*, a dimer formation with $q = (0.5, 0.0, 0.0)$ is stabilized over the non-dimerized state and opens a band gap, which suggests the possibility of the structural transition accompanying a metal-insulator transition³². More recent X-ray diffraction, as well as a high-resolution tunneling electron microscopy experiment, observed a structural modulation of the Te chain with $q_{CDW} = (0.4, 0.0, 0.5)$ as shown in Fig. 1(c)³³. The CDW transition in CuTe is also investigated utilizing angle-resolved photoemission spectroscopy (ARPES) and analyzed with first principles calculations³⁴. The momentum-dependent gap opening of 0.1-0.2 eV for a quasi 1D band is clearly observed below T_{CDW} in the ARPES signals. They also demonstrated the band structure evolution with temperature from 20 K to 350 K and potassium doping, and eventual disappearance of the CDW gap feature. Both Fermi surface nesting and electron-phonon coupling were reported as an origin of the CDW instability from a peak feature in the bare charge susceptibility and a Kohn anomaly in the phonon calculation at q_{CDW} . Their phonon dispersion curve, however, does not show the imaginary phonon frequency at q_{CDW} , which is the evidence of the structural instability³⁴.

To unveil the microscopic mechanism of the CDW transition, in this paper, we present the electronic structure and lattice dynamics of CuTe by first principles calculations. Especially, we focus on the Coulomb correlation of Cu ion because of its partial occupied d orbitals. We considered various types of van der Waals interaction scheme, exchange-correlation functionals, and electron-electron correlation strength to explore the origin of the modulation. Among them, we find that the strong Coulomb correlation of Cu d orbitals has an essential role in triggering the CDW transition. The phonon dispersion curve with considering the correlation effect provides the imaginary frequency whose corresponding lattice displacement is exactly consistent with the experimental Te modulation.

II. COMPUTATIONAL DETAILS

Density functional theory (DFT) calculations for structural relaxations and force calculations were performed by the Vienna *ab initio* simulation package, VASP³⁵. PHONOPY were used for phonon calculations³⁶. FPLO was employed to analyze the detailed band structure including band unfolding³⁷.

We included the spin-orbit coupling (SOC) and utilized two exchange-correlation functionals: Perdew-Burke-Ernzerhof functional (PBE)⁴⁰ and PBEsol (revised PBE for solid)⁴¹. We performed the PBE+ U calculations to account for the correlated d orbitals of Cu with the Du-

darev implementation³⁹. $U_{eff} = U - J$ in a range of 2 eV to 13 eV is tested to investigate the Coulomb correlation effect on the structural instability. Three different types of van der Waals interaction schemes are also checked: DFT-D3 method with zero-damping (D3)⁴² and Becke-Jonson damping (D3-BJ)⁴³, and D2 method of Grimme (D2)⁴⁴. The energy cut for the plane waves in the overall calculation is 400 eV. For the structural relaxations, the \mathbf{k} -point sampling for the non-CDW and the CDW structure are $20 \times 16 \times 8$ and $4 \times 16 \times 4$, respectively.

For the phonon calculation, the dynamical matrix is obtained with finite displacements method (frozen phonon method) using the $10 \times 1 \times 2$ supercell, based on the Hellmann-Feynman theorem^{36,45}. Before carrying out the phonon calculations, we performed the atomic relaxation using experimental lattice parameters³³. The \mathbf{k} -point sampling of $3 \times 16 \times 4$ is used for the $10 \times 1 \times 2$ supercell.

To obtain a reasonable range of Coulomb correlation parameters of Cu atoms, we have employed the linear response method⁴⁶ implemented in QUANTUM ESPRESSO³⁸. The dense ($48 \times 36 \times 24$) \mathbf{k} mesh is used for the high symmetric primitive unit cell. The energy cut for wavefunctions and the kinetic energy cut for charge density and potential are 45 Ry and 250 Ry, respectively.

III. RESULTS AND DISCUSSIONS

To investigate the instability of the Te chains, we relaxed the internal parameters of the $5 \times 1 \times 2$ supercell, starting from the experimental one³³ and obtained d_{min} and d_{max} (See Fig. 1) in Te chains in various simulation conditions employing diverse types of van der Waals interactions and functional, varying Coulomb correla-

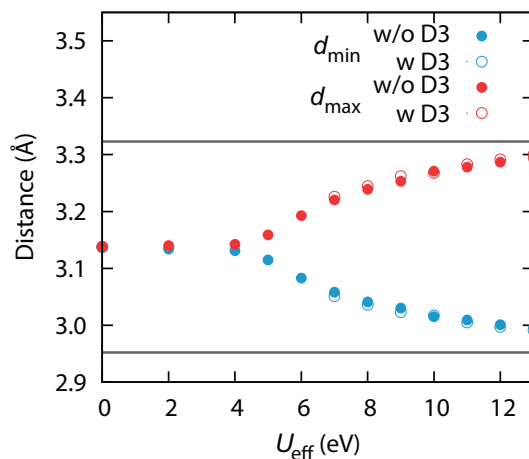


FIG. 2: Distances of the Te-Te bonding as a function of U_{eff} . The solid and dotted lines represent the distances after the relaxation without and with the van der Waals interaction with the D3 method, respectively. Gray lines indicate the experimental values.

functional	a	b	c	z_{Cu}	z_{Te}
PBE	3.280	4.018	7.457	0.466	0.242
PBEsol	3.197	3.949	6.921	0.463	0.222
PBE+vdW	3.170	3.996	6.919	0.457	0.219
PBE+D3+U9	3.081	4.035	6.986	0.455	0.220
PBE+D2+U9	3.093	4.338	6.950	0.452	0.219
PBE+D3-BJ+U9	3.074	4.010	6.830	0.455	0.214
PBE+U9	3.138	4.101	7.415	0.459	0.236
EXP*	3.138	4.059	6.902	0.454	0.221

TABLE I: Calculated lattice parameters and atomic positions of the non-CDW phase depending on the simulation condition. U9 means the U_{eff} of 9eV.

tion parameters (U_{eff}), and for hole doping case. The modulated CDW structure is relaxed back to the high-symmetric non-CDW structure losing the formation of the Te modulation except when the Coulomb correlation for Cu d orbitals is considered. This result is consistent with the stable phonon dispersion curve of Zhang *et al.*³⁴, where strong Coulomb correlation is not included.

Figure 2 shows the calculated d_{min} and d_{max} depending on the U_{eff} . As U_{eff} increases, clear bifurcation of d_{min} and d_{max} is observed, and their values are progressively reaching the experimental values regardless of the van der Waals correction. When the U_{eff} is larger than 9 eV, the differences between the calculated and the experimental d_{min} and d_{max} are less than 3 %. Previous papers have chosen the U value > 6.5 eV for Cu atom in copper oxides case^{47–51}. Furthermore, to ensure the reliability of our U_{eff} value, we performed the linear response method and obtained the self-consistent U_{eff} for Cu atoms of 11.5 eV, which agrees well with our finding in Fig. 2.

In addition, we performed full relaxation using the non-CDW structure as in Fig. 1(a) and (b). The lattice parameter c is reproduced well with the inclusion of van der Waals interaction and PBEsol functional as in Table I. However, other lattice parameters, a and b , and atomic positions do not considerably depend on the simulation conditions. Also, the scheme dependence of van der Waals correction is not significant. All calculated lattice parameters and atomic positions are comparable to the experimental values regardless of the condition.

The correlation effect of Cu d orbitals is investigated by observing the band dispersion and density of states (DOS) without(a) and with(b) U as in Fig. 3. The band dispersion dominated by Te p_x (σ bond along the a -axis) and p_y (π bond along the a -axis) near the Fermi level, E_f is hardly affected by the inclusion of U , however, the strong Cu weight redistribution to higher binding energy centering -5eV is observed, which suggests a non-negligible modification in Cu-Te hybridization near the

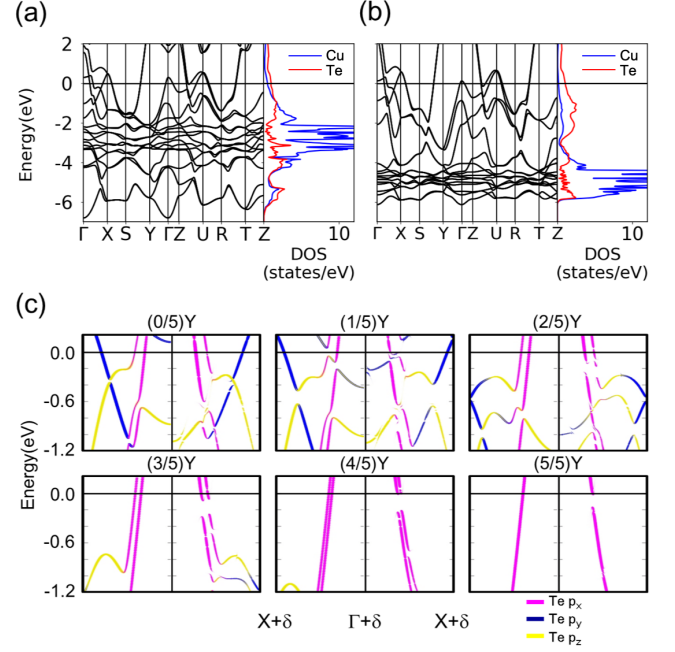


FIG. 3: Band structures and DOS of the non-CDW structure with (a) PBE and (b) PBE+ U . (c) Band unfolding data with the CDW structure. On each figure, a mirror image of high symmetry BS (left) is compared with CDW BS (right).

E_f . As a result, Te character becomes more pronounced at the E_f as in Fig. 3(b). The Cu weight shift from Fermi level can strengthen the 1D nature by removing Cu-Te hopping channel, which is a suitable condition for the CDW transition. Note that Cu bands are located in the range of -2 to -4 eV, and in the range of -4 to -6 eV in PBE and PBE+ U calculations, respectively. Thus, the experimental measurement of Cu weight might be interesting to check the correlation effect of Cu.

Figure 3(c) shows the modification in band structures with the Te modulation: six figures present unfolded band structures along Γ -X shifted by $\delta = \alpha Y$ ($\alpha = 0, 1/5, 2/5, 3/5, 4/5$, and 1), as in the supplementary of Ref. 34. The most announced change occurs in the Te p_x channel as expected. The band gap starts to open when $\alpha > 2/5$, which is consistent with the gap size dispersion along k_y in the previous experiment³⁴. The overall feature of Te weight agrees well with the experimental observation that the CDW band gap formed by Te p_x orbitals. In addition, our and previous unfolding data³⁴ require a slight shift in energy to match with the experimental results. This need for the shift in energy might come from the hole doping on the system. However, the CDW structure with hole doping was restored to the high symmetric non-CDW structure after structural relaxation without the inclusion of U , which discards the doping-derived CDW transition scenario.

Figure 4(a) and (b) show the phonon dispersion curves of the non-CDW state using PBE and PBE+ U , respectively. We did not include the SOC for the PBE

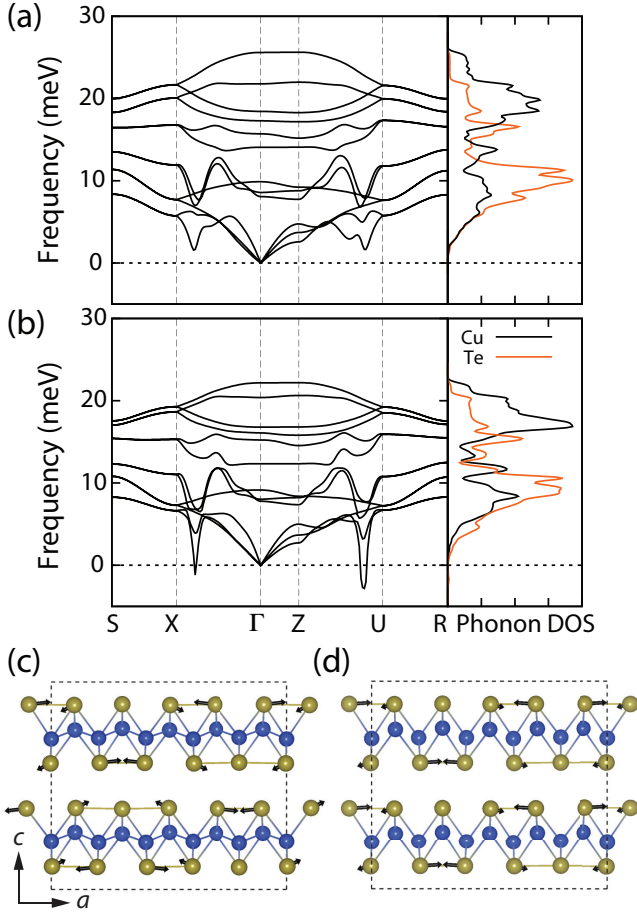


FIG. 4: Phonon dispersion curves and phonon DOSs of CuTe: (a) result from the PBE and (b) result from the PBE+ U . The imaginary phonon frequencies implies the structural instability. Lattice displacements by the phonon soft modes at (c) $q_{ph0} = (0.4, 0.0, 0.5)$ and (d) $q_{ph1} = (0.4, 0.0, 0.0)$.

case to compare with previous phonon calculations^{34,52}. The phonon structures of PBE+ U without SOC and PBE+ U +D3 are qualitatively the same with that of PBE+ U in Fig. 4(b), which show the imaginary phonon frequencies at $q_{ph0} = (0.4, 0.0, 0.5)$ and at $q_{ph1} = (0.4, 0.0, 0.0)$. The imaginary phonon frequency so-called phonon soft mode indicates the structural instability. This demonstrates the critical role of the Coulomb correlation of Cu d electrons in the CDW, which is consistent with structure relaxation results shown above. The phonon bands soften with the addition of the Coulomb correlation. Especially, as in the phonon DOSs of Fig. 4, while the Te and Cu phonon bands in the PBE result are similarly occupied at a low frequency range below 5 meV, the Te bands are more occupied and Cu bands are less occupied at the low frequency range in the PBE+ U calculation. The phonon DOSs show that with inclusion of U , Cu weight becomes decoupled in the low frequency region where the soft mode is located, which supports our weakened Cu-Te bonding scenario from the

electronic DOS analysis. It is worth noting that the correlation of Cu d adjusts not only Cu phonon bands but also Te phonon bands, leading to the imaginary phonon frequency of the Te phonon bands. The non-CDW structure exhibits a stable phonon dispersion curve in Fig. 4(a) (also reported by Zhang *et al.*³⁴) without consideration of the Coulomb correlation despite the experimentally unstable non-CDW structure at a low temperature. The correlation-assisted phonon soft mode and structural transition as in Fig. 4(b) has been reported in similar quasi-1D systems^{29,30}.

The phonon instability at q_{ph0} reproduces the experimental q_{CDW} . Figure 4(c) illustrates the lattice displacements of the softened phonon mode at q_{ph0} . This displacement of Te atoms generates $5 \times 1 \times 2$ modulation of Te chains, which are not captured in the previous phonon calculations^{34,52}. Our results demonstrate the electron-electron correlation and electron-phonon coupling play an essential role in driving the CDW. In addition, Figure 4(d) represents the corresponding lattice displacement of the phonon soft mode at q_{ph1} . It also contains the same Te-Te modulation in a layer but does not change along the c direction. The relaxed structure from q_{ph0} modulation has lower energy of 1.6 meV than that from q_{ph1} modulation. It explains why the CDW occurs at q_{ph0} not at q_{ph1} . The phonon instability is mostly related to the Te quasi-1D chain. And the small energy difference between q_{ph0} and q_{ph1} is related to chain-chain interaction which is the second order effect.

IV. CONCLUSIONS

In conclusion, we demonstrated that using DFT and phonon analysis, the Coulomb correlation of Cu 3d orbital plays an indirect but crucial role in the CDW transition of Te chains in the layered CuTe. We found that the inclusion of U pushes away Cu d orbitals from E_f to the higher binding energy region and accordingly weakens the Cu-Te bonding. This strengthens 1D nature of Te-Te bonding in the Te chain resulting in the CDW instability. Only with the inclusion of the Coulomb correlation in Cu atom, we observed the experimentally consistent imaginary phonon soft mode whose corresponding lattice distortion reproduces the CDW modulation. We believe that our work can shed light on the understanding of a mechanism of CDW transitions, especially when the interplay of multiple physical parameters are on effect.

Acknowledgments

We acknowledge the fruitful discussion with J. H. Shim and K.-T. Ko. This work was supported by the NRF Grant (Contracts No. 2016R1D1A1B02008461, No. 2017M2A2A6A01071297, No. 2018R1D1A1A02086051), Max-Planck POSTECH/KOREA Research Initiative (Grant No. 2016K1A4A4A01922028), and the KISTI su-

-
- * kyoo@mpk.or.kr
- ¹ Horst L. Stormer, *Rev. Mod. Phys.* **71**, 875 (1998).
 - ² C. Zeng, P. R. C. Kent, T.-H. Kim, A.-P. Li and H. H. Weitering, *Nat. Mater.* **7**, 539 (2008).
 - ³ K. S. Burch, D. Mandrus, J.-G. Park, *Nature* **563**, 47 (2018).
 - ⁴ K. Kim, J. Seo, E. Lee, K.-T. Ko, B. S. Kim, B. G. Jang, J. M. Ok, J. Lee, Y. J. Jo, W. Kang, J. H. Shim, C. Kim, H. W. Yeom, B. I. Min, B.-J. Yang and J. S. Kim, *Nat. Mater.* **17**, 794 (2018).
 - ⁵ M. Gibertini, M. Koperski, A. F. Morpurgo and K. S. Novoselov, *Nat. Nanotechnol.* **14**, 408 (2019).
 - ⁶ X. Chia and M. Pumera, *Nat. Catal.* **1**, 909 (2018).
 - ⁷ P. A. Lee, N. Nagaosa, and X.-G. Wen, *Rev. Mod. Phys.* **78**, 17 (2006).
 - ⁸ Y. Cao, V. Fatemi, S. Fang, K. Watanabe, T. Taniguchi, E. Kaxiras and P. Jarillo-Herrero, *Nature* **556**, 43 (2018).
 - ⁹ A. M. Gabovich, A. I. Voitenko, J. F. Annett and M. Ausloos, *Supercond. Sci. Technol.* **14**, R1 (2001).
 - ¹⁰ Xuetao Zhu, Yanwei Cao, Jiandi Zhang, E. W. Plummer, and Jiandong Gui, *PNAS* **112**, 2367 (2015).
 - ¹¹ Xuetao Zhu, Jiandong Gui, Jiandi Zhang, and E. W. Plummer, *Advances in Physics:X* **2**, 622 (2017).
 - ¹² F. Denoyer, R. Comes, A.F. Garito, and A. J. Heeger, *Phys. Rev. Lett.* **35**, (1975).
 - ¹³ D. Jérôme, *Chem. Rev.* **104**, 5555 (2004).
 - ¹⁴ Seiichi Kagoshima, Hiroyuki Anzai, Koji Kajimura, and Takehiko Ishiguro, *J. Phys. Soc. Japan* **39**, 1143 (1975).
 - ¹⁵ Sander van Smaalen, *Acta Cryst. A* **61**, 51 (2005).
 - ¹⁶ T. Sambongi, K. Tsutsumi, Y. Shiozaki, M. Yamamoto, K. Yamaya, and Y. Abe, *Solid State Commun.* **22**, 729 (1977).
 - ¹⁷ Z. Z. Wang, P. Monceau, H. Salva, C. Roucau, L. Guemas, and A. Meerschaut *Phys. Rev. B* **40**, 11589 (1989).
 - ¹⁸ F. W. Boswell, and A. Prodan, *Physica B* **99**, 364 (1980).
 - ¹⁹ J. P. Pouget, C. Noguera, A. H. Moudden, and R. Moret, *J. Phys. France* **46**, 1731 (1985).
 - ²⁰ R. M. Fleming, L. F. Schneemeyer, and D. E. Moncton, *Phys. Rev. B* **31**, 899 (1985).
 - ²¹ Andrea Decker, Gregory A. Landrum, and Richard Dronskowski, *Z. Anorg. Allg. Chem.* **628**, 295 (2002).
 - ²² B. I. Min, J. H. Shim, Min Sik Park, Kyoo Kim, S. K. Kwon, and S. J. Youn, *Phys. Rev. B* **73**, 132102 (2006).
 - ²³ M. D. Johannes and I. I. Mazin, *Phys. Rev. B* **77**, 165135 (2008).
 - ²⁴ D. Kartoon, U. Argaman, and G. Makov, *Phys. Rev. B* **98**, 165429 (2018).
 - ²⁵ Eric Jeckelmann, *Phys. Rev. B* **57**, 11838 (1998).
 - ²⁶ P. Sengupta, A. W. Sandvik and D. K. Campbell, *Phys. Rev. B* **67**, 245103 (2003).
 - ²⁷ S. Biermann, A. Poteryaev, A. I. Lichtenstein, and A. Georges, *Phys. Rev. Lett.* **94**, 026404 (2005).
 - ²⁸ M. W. Haverkort, Z. Hu, A. Tanaka, W. Reichelt, S. V. Streltsov, M. A. Korotin, V. I. Anisimov, H. H. Hsieh, H.-J. Lin, C. T. Chen, D. I. Khomskii, and L. H. Tjeng, *Phys. Rev. Lett.* **95**, 196404 (2005).
 - ²⁹ S. Kim, K. Kim, C.-J. Kang and B. I. Min *Phys. Rev. B* **87**, 195106 (2013).
 - ³⁰ S. Kim, K. Kim and B. I. Min *Phys. Rev. B* **90**, 045124 (2014).
 - ³¹ F. Pertlik, *Minealogy and Petrology* **71**, 149 (2001).
 - ³² S. Seong, T. A. Albright, X. Zhang and M. Kanatzidis, *J. Am. Chem. Soc.* **116**, 7287 (1994).
 - ³³ K. Stolze, A. Isaeva, F. Nitsche, U. Burkhardt, H. Lichte, D. Wolf and T. Doert, *Angew. Chem Int. Ed.* **52**, 862 (2013).
 - ³⁴ Kenan Zhang, Xiaoyu Liu, Haoxiong Zhang, Ke Deng, Mingzhe Yan, Wei Yao, Mingtian Zheng, Eike F. Schwier, Kenya Shimada, Jonathan D. Denlinger, Yang Wu, Wenhui Duan, and Shuyun Zhou, *Phys. Rev. Lett.* **121**, 206402 (2018).
 - ³⁵ G. Kresse and J. Furthmüller, *Phys. Rev. B* **54**, 11169 (1996); *Comput. Mater. Sci.* **6**, 15 (1996).
 - ³⁶ A. Togo, F. Oba, and I. Tanaka, *Phys. Rev. B* **78**, 134106 (2008).
 - ³⁷ W. Ku, T. Berlijn, and C.-C. Lee. *Phys. Rev. Lett.* **104**, 216401 (2010).
 - ³⁸ P. Giannozzi, S. Baroni, N. Bonini, M. Calandra, R. Car, C. Cavazzoni, D. Ceresoli, G. L. Chiarotti, M. Cococcioni, I. Dabo, A. Dal Corso, S. Fabris, G. Fratesi, S. de Gironcoli, R. Gebauer, U. Gerstmann, C. Gougousis, A. Kokalj, M. Lazzeri, L. Martin-Samos, N. Marzari, F. Mauri, R. Mazzarello, S. Paolini, A. Pasquarello, L. Paulatto, C. Sbraccia, S. Scandolo, G. Schlauro, A. P. Seitsonen, A. Smogunov, P. Umari, R. M. Wentzcovitch, *J. Phys.:Condens. Matter*, **21**, 395502 (2009).
 - ³⁹ S. L. Dudarev, G. A. Botton, S. Y. Savrasov, C. J. Humphreys, and A. P. Sutton, *Phys. Rev. B* **57**, 1505 (1998).
 - ⁴⁰ J. P. Perdew, K. Burke, and M. Ernzerhof, *Phys. Rev. Lett.*, **77** 3865 (1996).
 - ⁴¹ J. P. Perdew, A. Ruzsinszky, G. I. Csonka, O. A. Vydrov, G. E. Scuseria, L. A. Constantin, X. Zhou, and K. Burke, *Phys. Rev. Lett.* **100** 136406 (2008).
 - ⁴² S. Grimme, J. Antony, S. Ehrlich and S. Krieg, *J. Chem. Phys.* **132**, 154104 (2010).
 - ⁴³ S. Grimme, S. Ehrlich, and L. Goerigk, *J. Comp. Chem.* **32**, 1456 (2011).
 - ⁴⁴ S. Grimme, *J. Comp. Chem.* **27**, 1787 (2006).
 - ⁴⁵ K. Parlinski, Z. Q. Li, and Y. Kawazoe, *Phys. Rev. Lett.* **78**, 4063 (1997).
 - ⁴⁶ M. Cococcioni and S. de Gironcoli, *Phys. Rev. B* **71**, 035105 (2005).
 - ⁴⁷ V.I. Anisimov, J. Zaanen, and O.K. Andersen, *Phys. Rev. B* **44**, 943 (1991).
 - ⁴⁸ C.E. Ekuma, V.I. Anisimov, J. Moreno and M. Jarrell *Eur. Phys. J. B* **87**, 23 (2014).
 - ⁴⁹ M. Nolan and S.D. Elliott *Phys. Chem. Chem. Phys.*, **8**, 5350 (2006).
 - ⁵⁰ I. S. Elfimov, G. A. Sawatzky and A. Damascelli, *Phys. Rev. B*, **77**, 060504(R) (2008).
 - ⁵¹ A. K. Mishra, A. Roldan and N. H. de Leeuw *J. Phys. Chem. C* **120**, 2198 (2016).
 - ⁵² J. U. Salmón-Gamboa, A. H. Barajas-Aguilar, L. I. Ruiz-Ortega, A. M. Garay-Tapia, and S. J. Jiménez-Sandoval *Sci. Rep.* **8**, 8093 (2018).